catalysts

MDPI

Supplementary Materials

Molecular Insights into Substrate Binding of the Outer Membrane Enzyme OmpT

Yubo Zhang [1] and Marc Baaden [2,*]

[1] Department of Food Science, Foshan University, Foshan 528231, China
[2] Université Paris Cité, CNRS, Laboratoire de Biochimie Théorique, 13 rue Pierre et Marie Curie, F-75005 Paris, France
* Correspondence: baaden@smplinux.de; Tel.: +33-1-58-41-51-76

Abstract: This document contains supplementary data for the above-mentioned manuscript published in the journal catalysts.

Keywords: molecular dynamics simulations; outer membrane protease OmpT; substrate recognition

S2. Supplementary Results

S2.7 Free energy profiles from umbrella sampling MD simulations characterize the driving force for association

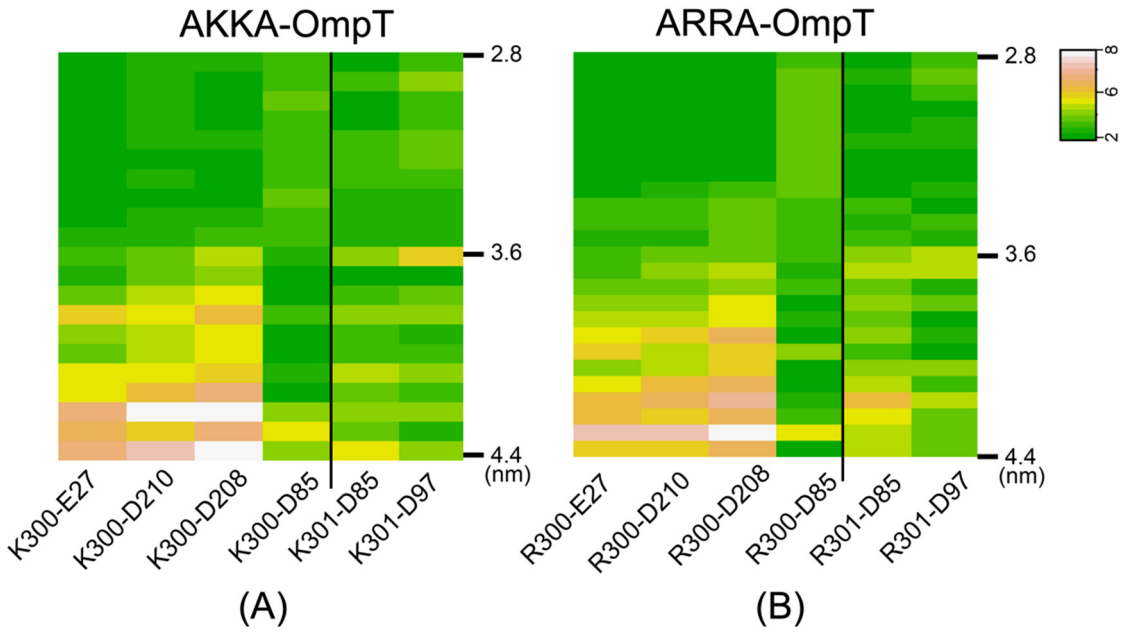

Figure S1. Closest contact distances of salt bridges between selected active site residues (E27, D210, D208, D85 and D97) of OmpT and basic residues at positions 300 and 301 of the AKKA (**A**) and ARRA (**B**) peptides as a function of the z reaction coordinate used during umbrella sampling for the extraction of the substrate from the active site. The distance of salt bridges was calculated using the smallest native distance between two residues.

S2.8 A search for putative catalytic water molecules yields two candidate poses

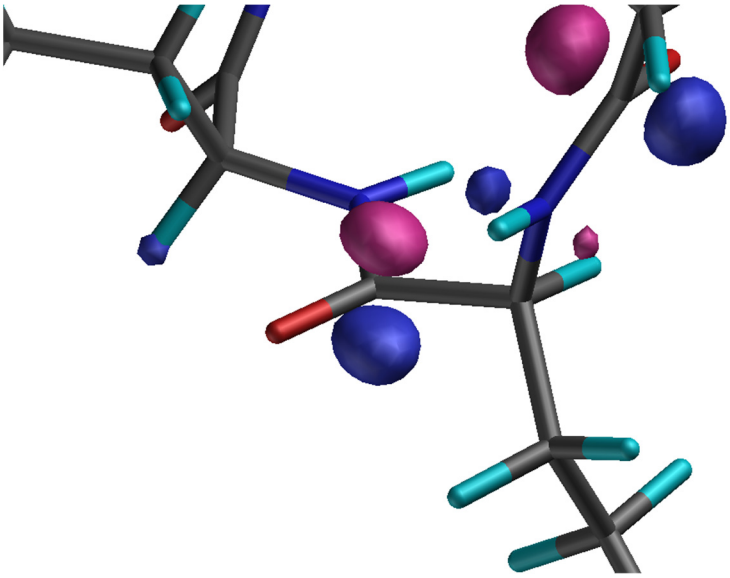

Figure S2. Results of an extended Hückel calculation, a simplified method for calculating the electronic structure of conjugated molecules, for the ARRA peptide in a docked formation, showing that the LUMO is located at the carbon atom of the central C=O in the peptide bond. The preferred attack would be from "below", e.g., from the direction of HIS212. In this structure, the distance from HIS -NE2 to LYS -C is 4.86 A. Interestingly, in a random structure of the peptide, the LUMO is not located at this peptide bond. Thus, the location of the orbital appears to be conformation dependent, and the approximately docked conformation appears to favor attack on the central peptide bond. The calculated LUMO (N=88) is shown, plotted at 0.03 a.u. The actual calculation was reported previously in ref [13].

S2.9 Lipid–protein interactions may specifically anchor OmpT within the membrane

We measured the convergence of lipid bilayer equilibration in the simulations by calculating the time series of the area per lipid (supplemental Figure S3) and the density profiles (supplemental Figure S4) of the membrane components during the MD simulations. The area per lipid for DMPC stabilized just below 0.65 nm^2 in both systems, which correlates well with experimental data [63]. Supplementary Fig. S4 shows the density profiles of the membrane components consisting of the head group, glycerol esters, and acyl chains, illustrating the expected distribution.

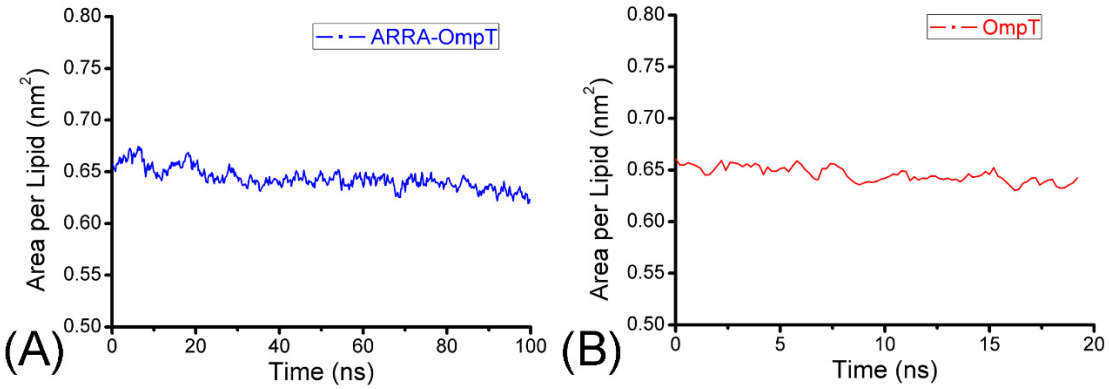

Figure S3. Area per lipid relaxation over time for the DMPC bilayer. The plots were obtained from the trajectories of (A) DMPC+ARRA/OmpT, and (B) DMPC+ OmpT.

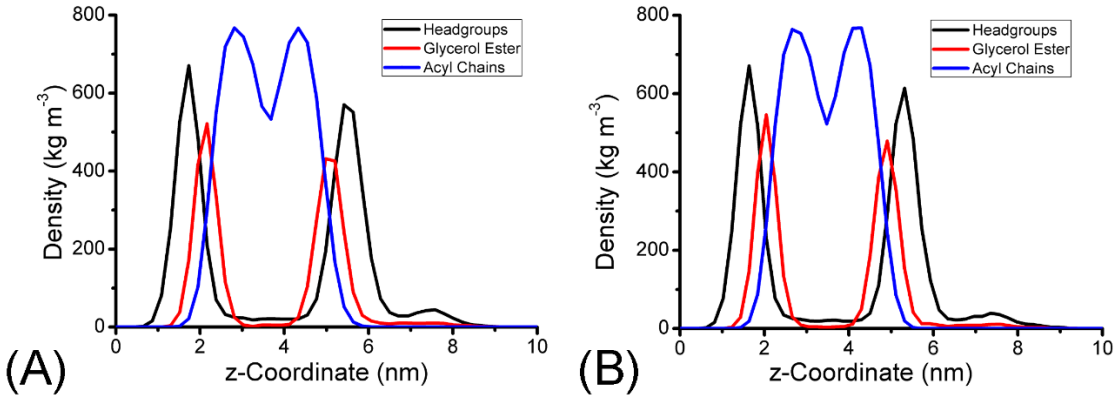

Figure S4. Density profiles of membrane components (headgroups, glycerol ester and acyl chains) along the membrane normal direction. The plots obtained from the trajectories of (**A**) DMPC+ARRA/OmpT, and (**B**) DMPC+ OmpT are shown.

We measured the number of interactions of DMPC lipids surrounding the ARRA-OmpT complex as a function of time. An interaction was defined when the distance between lipids and protein was closer than 3.5 Å. Fig. 8A shows that the number of DMPC lipids near OmpT is stable and fluctuates around 35, indicating convergence of lipid interactions during the simulation. Next, we divided the lipids into polar head groups and hydrophobic tail groups, and observed the contacts between lipid and protein atoms. Fig. 8B shows that the number of contacts of the tail groups varies around 100. For the head groups, the number of interactions gradually increases during the first 30ns of the simulation and stabilizes at 270 contacts, indicating a large number of interactions.

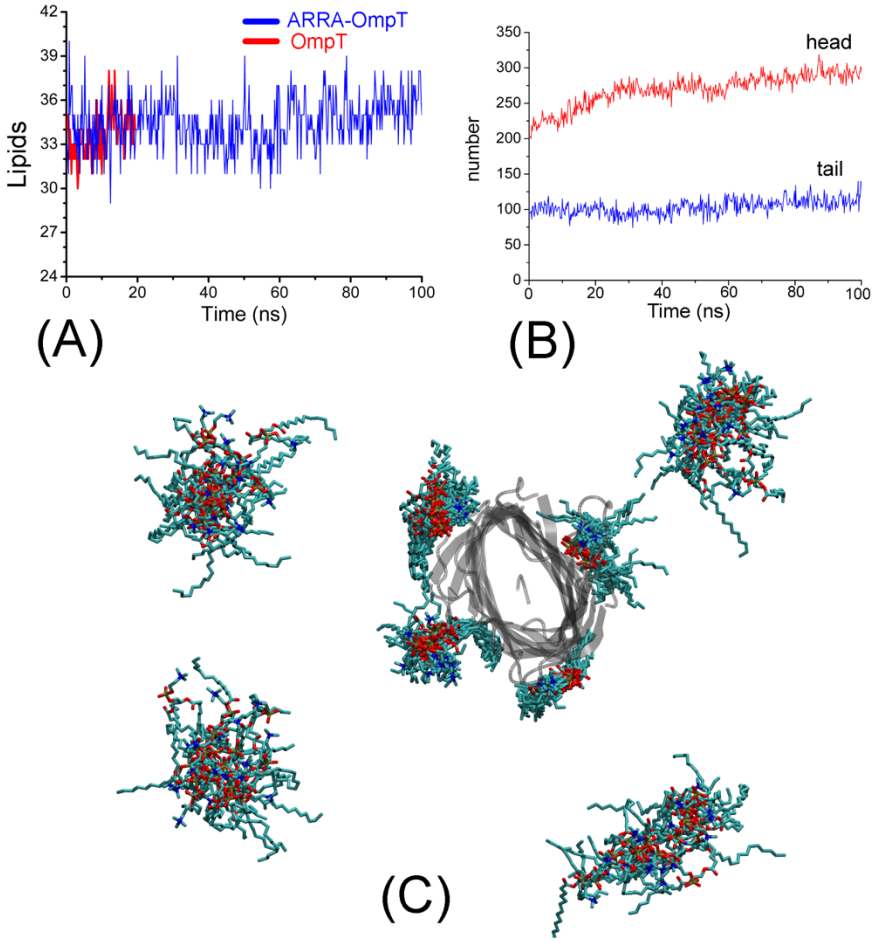

Figure S5. (**A**) Number of DMPC lipids contacting OmpT in the *apo* enzyme (34 lipid molecules) and *holo* enzyme systems (35 lipid molecules). (**B**) Number of DMPC atoms in contact with OmpT. The red line describes the number of contacts of the lipid head group (270 atoms), the blue line those of the lipid tails (104 atoms). (**C**) Cumulative view of some bound and free lipids (defined in the text) during the simulation (saved every 5 ns).

To better understand the effects of the membrane protein on the bilayer, we investigated the mobility of lipids during the MD simulation. Lipids were divided into two classes: 1) bound lipids, whose atoms are closer than 3.5 Å from OmpT throughout the simulation; 2) free lipids, whose atoms are never within 3.5 Å of the membrane protein. Supplementary Fig. 4 shows snapshots of free and bound lipids selected every 5ns. Qualitatively, it can be seen that bound lipids have a much more restricted position, while free lipids have a broad distribution of positions in the bilayer plane. This observation suggests that free lipids have higher lateral diffusion compared to bound lipids. To quantify relative lipid mobility, we measured lateral diffusion for both lipid classes. The diffusion coefficient was calculated in the first 10 ns, 15 ns, and 20 ns for *apo* OmpT and in the first 50 ns, 75 ns, and 100 ns for the ARRA-OmpT complex. Supplementary Table 1 shows that free lipids consistently exhibit a higher diffusion coefficient than bound lipids in both the *apo* enzyme and *holo* enzyme systems. The difference in mobility between bound and free lipids in our DMPC/OmpT system is in good agreement with previous studies on the DMPC/OmpA system [29], in which bound lipids have a diffusion coefficient approximately half that of free lipids.

Table S1. Lateral diffusion coefficients for lipids in the bilayer.

	Lateral Diffusion Coefficient ($10^{-5}cm^2s^{-1}$) [1]	
	Bound	**Free**
OmpT		
0–10ns	0.030 (±0.005)	0.047 (±0.013)
0–15ns	0.019 (±0.003)	0.038 (±0.008)
0–20ns	0.009 (±0.001)	0.029 (±0.010)
ARRA-OmpT		
0–50ns	0.037 (±0.006)	0.060 (±0.024)
0–75ns	0.023 (±0.004)	0.037 (±0.014)
0–100ns	0.020 (±0.003)	0.035 (±0.009)

[1]The lateral diffusion coefficient was calculated from the mean squared displacements of two classes of DMPC lipids for each individual molecule (bound lipids and free lipids) by linear regression [29].

Lipopolysaccharide (LPS) is essential for OmpT enzyme activity [64,65], although recent studies provide a more nuanced view [66]. We then analyzed the major contacts between the DMPC and the proposed LPS binding site (Tyr134, Glu136, Arg138, Arg175, and Lys226) of ARRA-OmpT (Supplementary Table 2). Our results showed the obvious H-bonds between the DMPC molecules and residues in the proposed LPS binding site in both *holo* enzyme and *apo* enzyme simulations, except for residue Tyr134. The H-bonds between Lys177 of the *holo* enzyme and the DMPC also indicate its important role in the binding site. The other contacts between the residues of the binding site of the *holo* enzyme and DMPC are in good agreement with those of the *apo* enzyme.

Table S2. Dominant lipid/protein interactions.

Interaction	ARRA-OmpT[1]	OmpT[1,3]
Proposed site		
Arg138	93.2	85.4
Arg175	60.5	33.3
Lys226	21.6	91
Tyr134	0.2	0
E136-w[2]	12.4	92.2
Vicinity		
Lys177	87.8	46.3
2nd site		
Arg77	93.8	95.4
Arg255	99.8	76.8
Asn47	100.0	100
Lower belt		
Tyr189	90.0	94.2
Tyr126	84.2	98.2
Thr2	92.6	36.1

[1] Values indicate the percentage of the total simulation time that a given lipid/protein interaction was present. [2] E136-w" represents residue E136 interacting with the lipid, possibly via a water molecule. Following [13], we define a group consisting of water molecules within 4 Å of the residue and the residue itself to calculate the interactions with DMPC. [3] Reference data on *apo* OmpT is taken from [13].

The protein–lipid interactions are defined as the percentage of total simulation time in which at least one H-bonding interaction is formed between the phosphate of DMPC and a protein side chain. The interactions for ARRA-OmpT and for OmpT were calculated from the 100 ns simulation of the *holo* enzyme and from the previously published 10 ns simulation of the *apo* enzyme [13]. Residues are listed for the proposed site, the surrounding site, the second site, and the lower belt, which were defined previously [13].

S3. Discussion

To explore and uncover the role of electrostatics, we performed a standard calculation of the electrostatic field of OmpT using a Poisson–Boltzmann approach with the APBS software [67]. We then visualized the results as field lines in our UnityMol visualization software [24]. The resulting animation can be found in Supplementary Video S1.

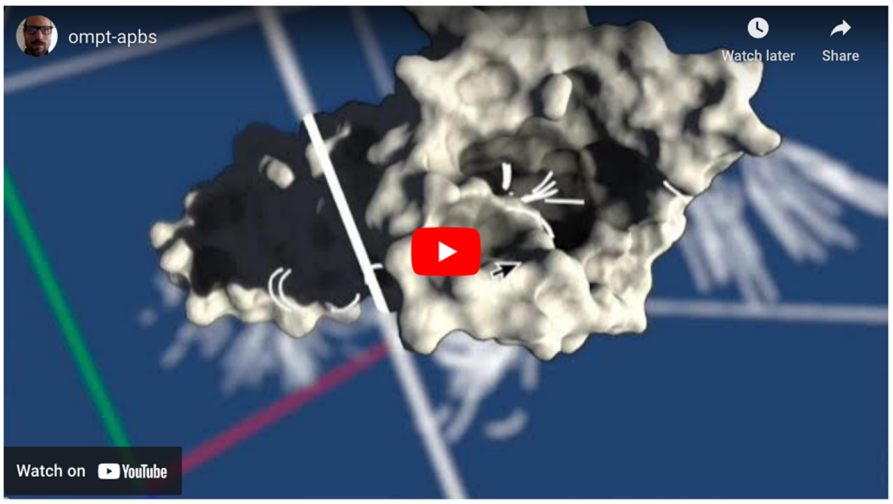

Video. S1. Animation of OmpT electrostatic field lines, accessible via https://www.youtube.com/watch?v=aFbD4MRA21A.

S4. Materials and Methods

Generation of atomic models

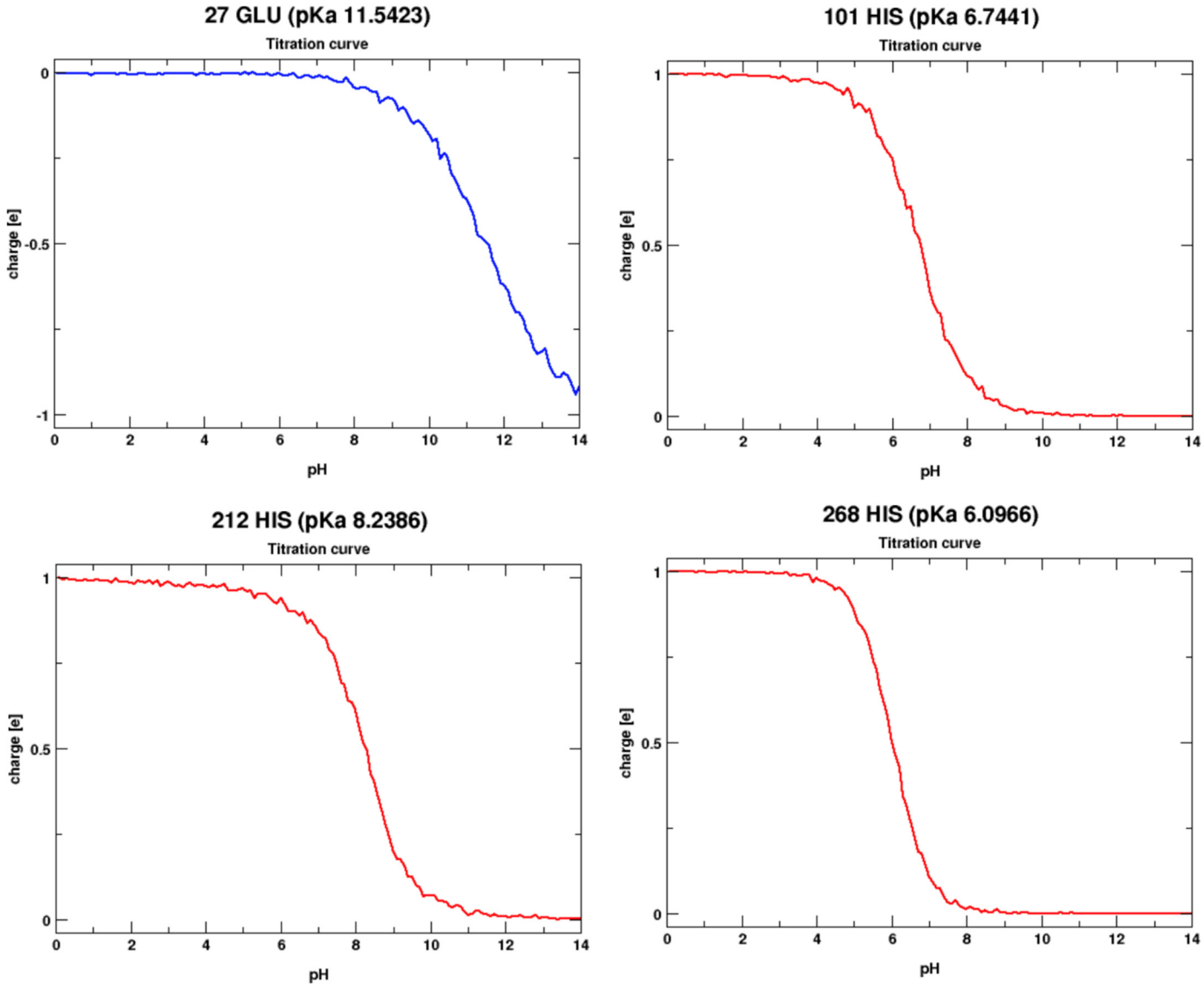

Figure S6. Titration curves for the four residues E27, H101, H212 and H238 with a predicted non-standard ionization state at pH7.

Table S3. Results for pKa calculations of OmpT in vacuo ("Bare) or in a membrane dielectic ("Slab").

Residue	Model	Bare	Slab	State (pH 7)
1 SER	8	8.4	7.8	prot +1
3 GLU	4.4	4.2	4.5	depr -1
10 ASP	4	4.5	4.8	depr -1
15 ASP	4	0	0	depr -1
24 LYS	10.4	12.6	12.5	prot +1
26 LYS	10.4	10.6	9.9	prot +1
27 GLU	4.4	11.5	19.8	**prot 0**
28 ARG	13	18.1	17.7	prot +1
30 TYR	9.6	9.1	11.1	prot 0
33 GLU	4.4	3.9	3.5	depr -1
34 GLU	4.4	3.4	4.3	depr -1
37 ARG	13	16.9	17.2	prot +1
38 LYS	10.4	10.9	10.7	prot +1
43 ASP	4	0.5	0.2	depr -1
45 LYS	10.4	10.7	10.3	prot +1
53 LYS	10.4	14.6	0	prot +1
59 ASP	4	0.9	0	depr -1
77 ARG	13	14.1	14.5	prot +1
83 ASP	4	3.4	3.5	depr -1 (slab+)
85 ASP	4	5.5	6.6	depr -1 (slab+)
88 ASP	4	2.7	1.8	depr -1
97 ASP	4	2.4	1.8	depr -1
98 GLU	4.4	1.4	1.4	depr -1
100 ARG	13	16.9	17.3	prot +1
101 HIS	6.3	6.7	5.7	depr 0
103 ASP	4	3.1	3.1	depr -1
108 TYR	9.6	9	9.5	prot 0
111 GLU	4.4	4.2	3.3	depr -1
113 ASP	4	0.1	0	depr -1
117 LYS	10.4	11.7	15.1	prot +1
123 GLU	4.4	3.8	3.9	depr -1
126 TYR	9.6	10.6	11.7	prot +1
127 ARG	13	17.4	19.6	prot +1
134 TYR	9.6	11.7	0	prot 0
136 GLU	4.4	2	0	depr -1
138 ARG	13	14	14.2	prot +1
139 TYR	9.6	13.2	18.7	prot 0
144 ARG	13	14.9	14.7	prot +1
148 TYR	9.6	11.3	11.6	prot 0
150 TYR	9.6	13.1	14	prot 0
153 GLU	4.4	5.4	5.8	,depr -1
154 GLU	4.4	4.8	4.8	depr -1
157 ARG	13	15.2	15.9	prot +1
158 ASP	4	2.3	1	depr -1
159 ASP	4	4.7	4.7	depr -1
167 GLU	4.4	4.2	4.1	depr -1
168 ARG	13	17.9	19	prot +1
172 TYR	9.6	0	0	prot 0
173 LYS	10.4	11.4	10.2	prot +1
175 ARG	13	16.4	0	prot +1
177 LYS	10.4	10.3	7.6	prot +1 (slab)
180 TYR	9.6	13	0	prot 0
187 TYR	9.6	10.3	12.6	prot 0
188 ARG	13	17.6	19.4	prot +1
189 TYR	9.6	10.5	11.6	prot 0
190 GLU	4.4	4.5	4.6	depr -1
191 ASP	4	3.8	4	depr -1
193 GLU	4.4	1.3	0.7	depr -1
199 LYS	10.4	0	0	prot +1
200 TYR	9.6	10.5	18.3	prot 0
205 GLU	4.4	2.2	1.4	depr -1
208 ASP	4	2.9	1.6	depr -1
210 ASP	4	0.6	5.5	depr -1 (slab)
211 GLU	4.4	2.4	3.4	depr -1
212 HIS	6.3	8.2	7.9	**prot +1 (slab)**
213 TYR	9.6	10.4	10.9	prot 0
214 ASP	4	1.9	1.7	depr -1
217 LYS	10.4	13.5	13.5	prot +1
218 ARG	13	15.9	17.9	prot +1
221 TYR	9.6	15	16.1	prot 0
222 ARG	13	17.2	17.8	prot +1
224 LYS	10.4	11.5	11.7	prot +1
226 LYS	10.4	10.6	10.9	prot +1
227 ASP	4	3.4	4.8	depr -1
230 TYR	9.6	15.5	0	prot 0
231 TYR	9.6	9.7	14.5	prot 0
239 TYR	9.6	10.8	13	prot 0
240 TYR	9.6	13.2	16.8	prot 0
246 LYS	10.4	15.4	14	prot +1
248 TYR	9.6	13	0	prot 0
250 GLU	4.4	2	0	depr -1
255 ARG	13	15.5	17.6	prot +1
259 LYS	10.4	12.2	12.7	prot +1
260 LYS	10.4	11.7	11.5	prot +1
266 TYR	9.6	10.7	11.2	prot 0
267 ASP	4	3.3	3.3	depr -1
268 HIS	6.3	6.1	5.2	depr 0
274 ASP	4	4.3	4.6	depr -1
275 TYR	9.6	9.5	10	prot 0
277 LYS	10.4	10.4	10.3	prot +1
283 GLU	4.4	0.6	0	depr -1
285 TYR	9.6	9.1	8.6	prot 0
294 LYS	10.4	11.2	10.6	prot +1
295 TYR	9.6	10.4	13.8	prot 0
297 PHE	3.8	4.5	5.2	depr -1

The residue column indicates the residue number and type, the model column indicates the standard pKa value for a given residue, the bare column indicates predicted pKa for OmpT in vacuo, the slab column indicates predicted pKa for OmpT in a dielectric medium such as a membrane and the state column indicates the most probable protonation state at pH7, prot for protonated, depr for deprotonated.